Identification and Characterization of Tropical Atmospheric Cold Pools using Space-borne Scatterometer, Precipitation and Modeling

Piyush Garg[1], Stephen W. Nesbitt[1], Timothy J. Lang[2], George Priftis[3], Jeffrey D. Thayer[1], Deanna A. Hence[1]

[1]University of Illinois Urbana Champaign

[2]NASA Marshall Space Flight Center, Alabama

[3]University of Alabama, Huntsville

Motivation

- Cold pool tracking and representation is an arduous task as they intersect and new cold pools form on their boundaries (Tompkins 2001; Feng et al., 2015).
- We aim to get a deeper insight into the evolution of tropical oceanic cold pools to better characterize the multi-scale tropical storm dynamics.
- Cold pools from older thunderstorms can merge into a mesoscale cold pools and can initiate secondary convection as observed in MCSs (Fujita, 1969; Johnson and Hamilton, 1988).
- ***Therefore we are trying to create a new identification metric to better identify these cold pools and their storm environments over tropics.***
- We are also matching the ASCAT overpasses with TRMM and GPM-IMERG precipitation in combination with MERRA-2 reanalysis products to get a holistic perspective of cold pools over oceans.

Gradient Features (GFs) Identification

- The hypothesis lies on identifying closed areas of steep gradients in horizontal winds, termed as Gradient Features (GFs).

$$|\nabla\vec{V}| = \begin{bmatrix} \frac{\partial u}{\partial x} + \frac{\partial v}{\partial x} \\ \frac{\partial u}{\partial y} + \frac{\partial v}{\partial y} \end{bmatrix}$$

- We have developed a new storm-centric, tensor-based approach to identify horizontal wind gradient.

- The figure shows two examples of cold pools that can be identified from ASCAT, (a) MCS and (b) shallow cumulus cloud clusters.

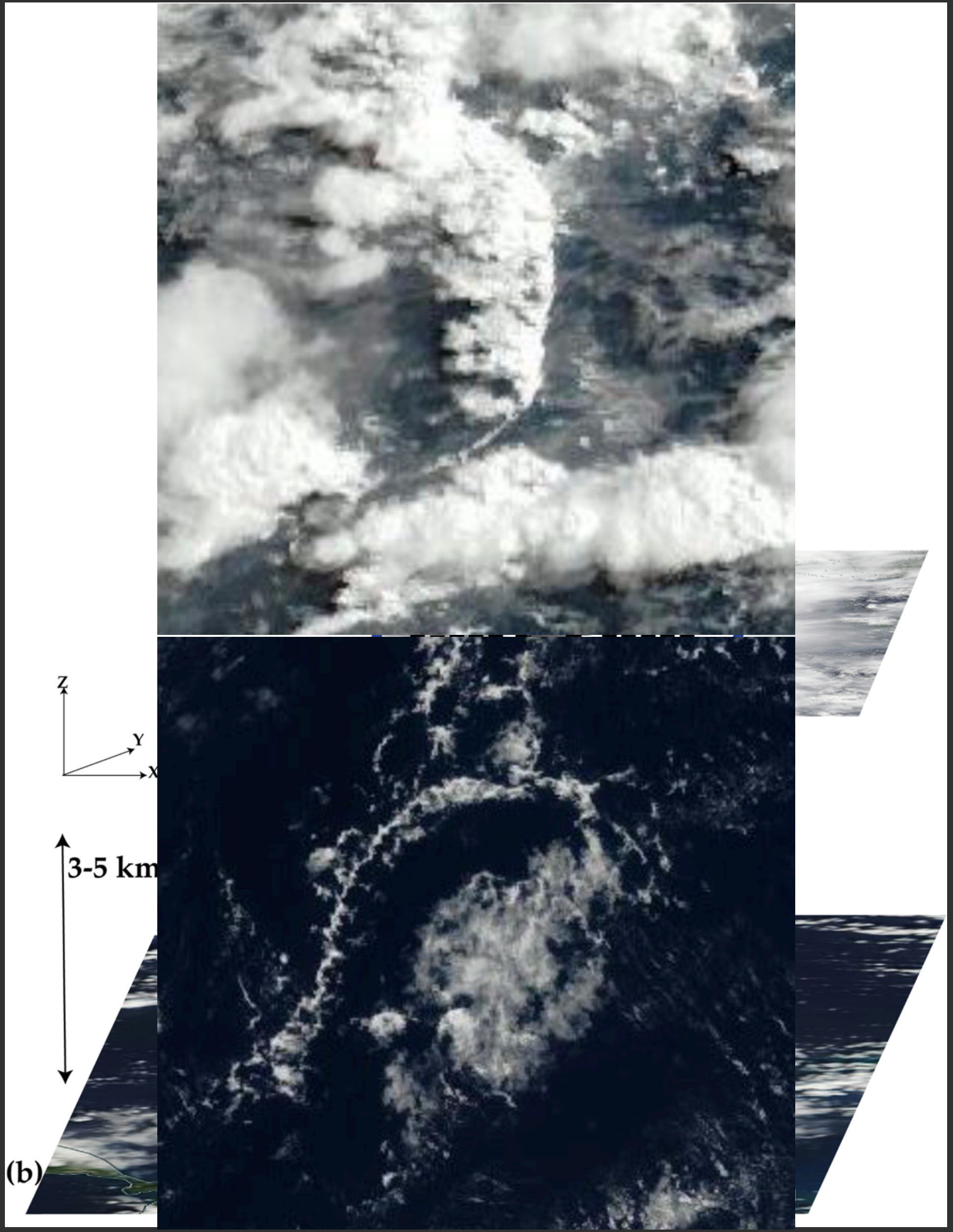

Gradient Feature Identification Algorithm Version 2.0

Calculate Horizontal Wind Gradient

- Using numpy convolve2d, first derivative of zonal and meridional wind is calculated

Label the feature using regionprops

- Scipy regionprops was used to label each feature satisfying the given threshold

Remove all the features having less than 4 pixels

- Remove all the features having less than 4 pixels to create a well-connected polygon

Apply Delaunay Triangulation

- Delaunay triangulation was applied to subdivide the irregular polygon into individual triangles

Apply the concept of α shapes

- Applying the α shape function to connect the perimeters of triangles to get the edges of the polygon

Identify Concave Hull

- **Voila! You have your Gradient Feature**

Example of GF on 22 May 2018

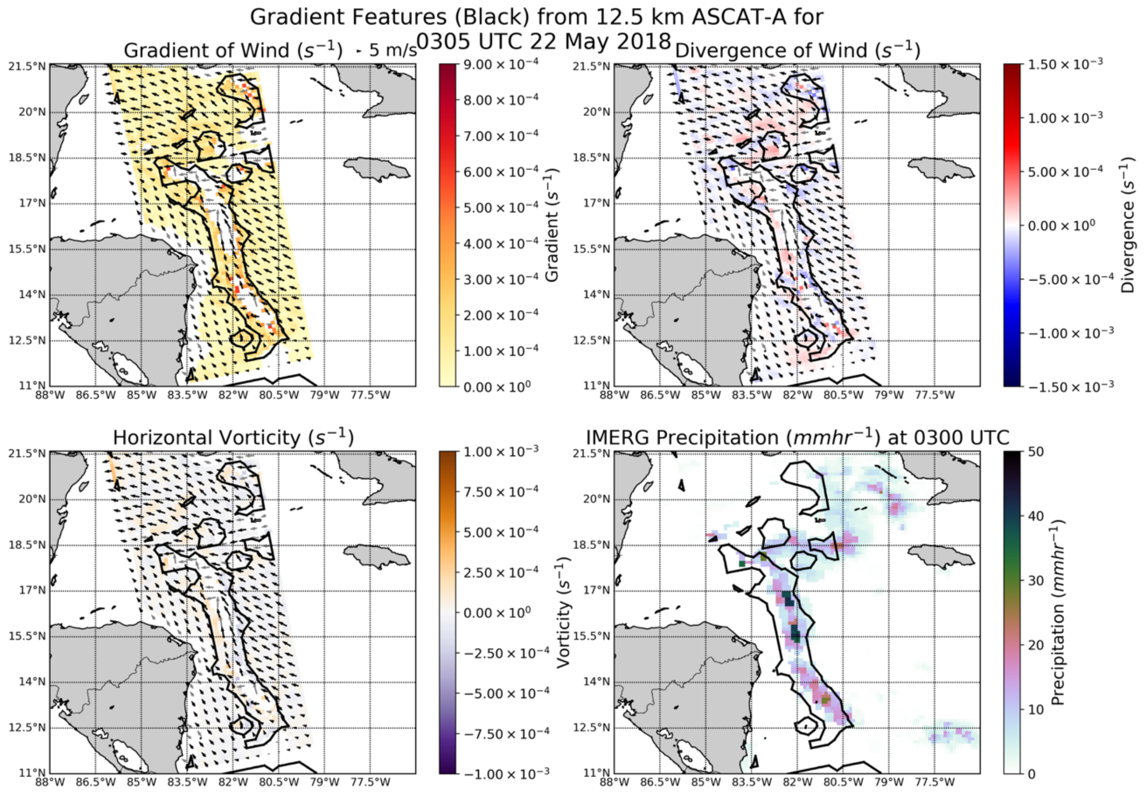

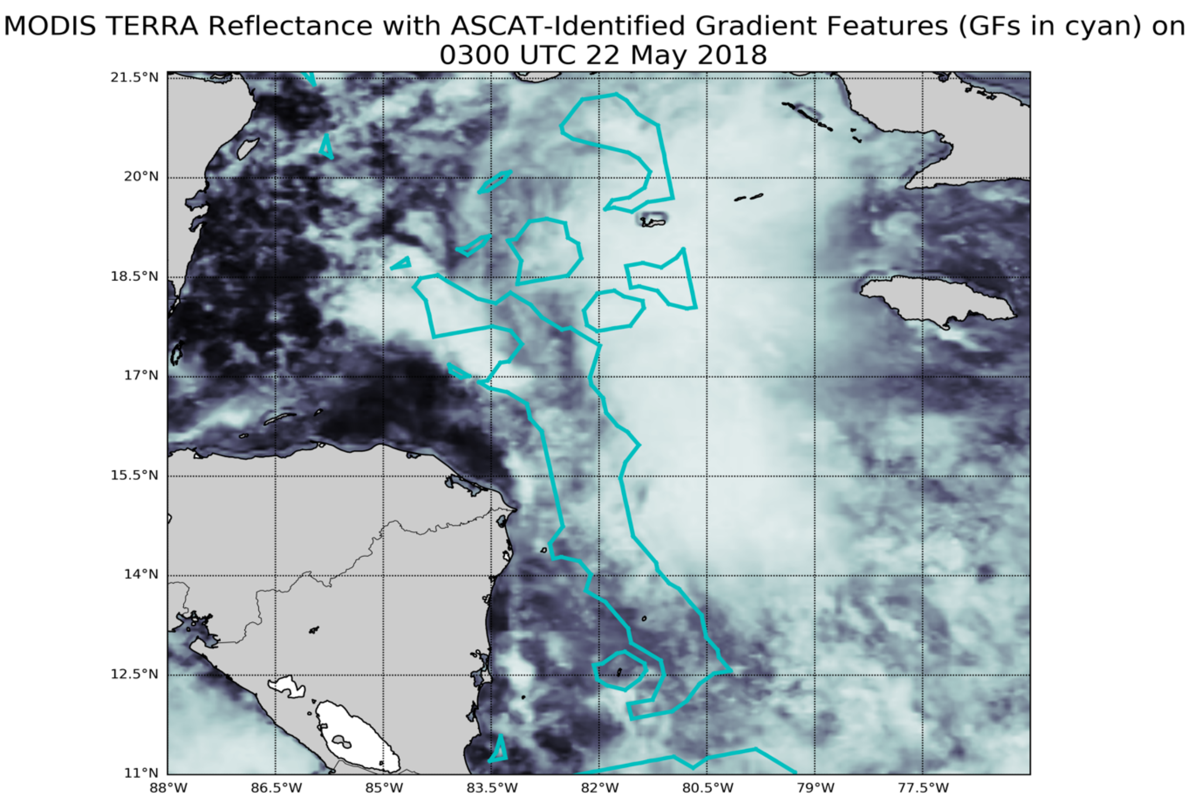

WRF-ARW Validation of GF Thresholds

- WRF v4.0 simulated 9-km data regridded to 12.5 km was used to validate the threshold and the performance of GF technique.
- The model ran for 15 days (00Z 17 October 2011 to 18Z 01 November 2011 during active MJO period.
- FFT filtered T_v anomaly threshold of -1.5 K was used to identify thermal cold pools in the model.
- GF-identified cold pools were then tested against thermal cold pools to obtain various success indices.

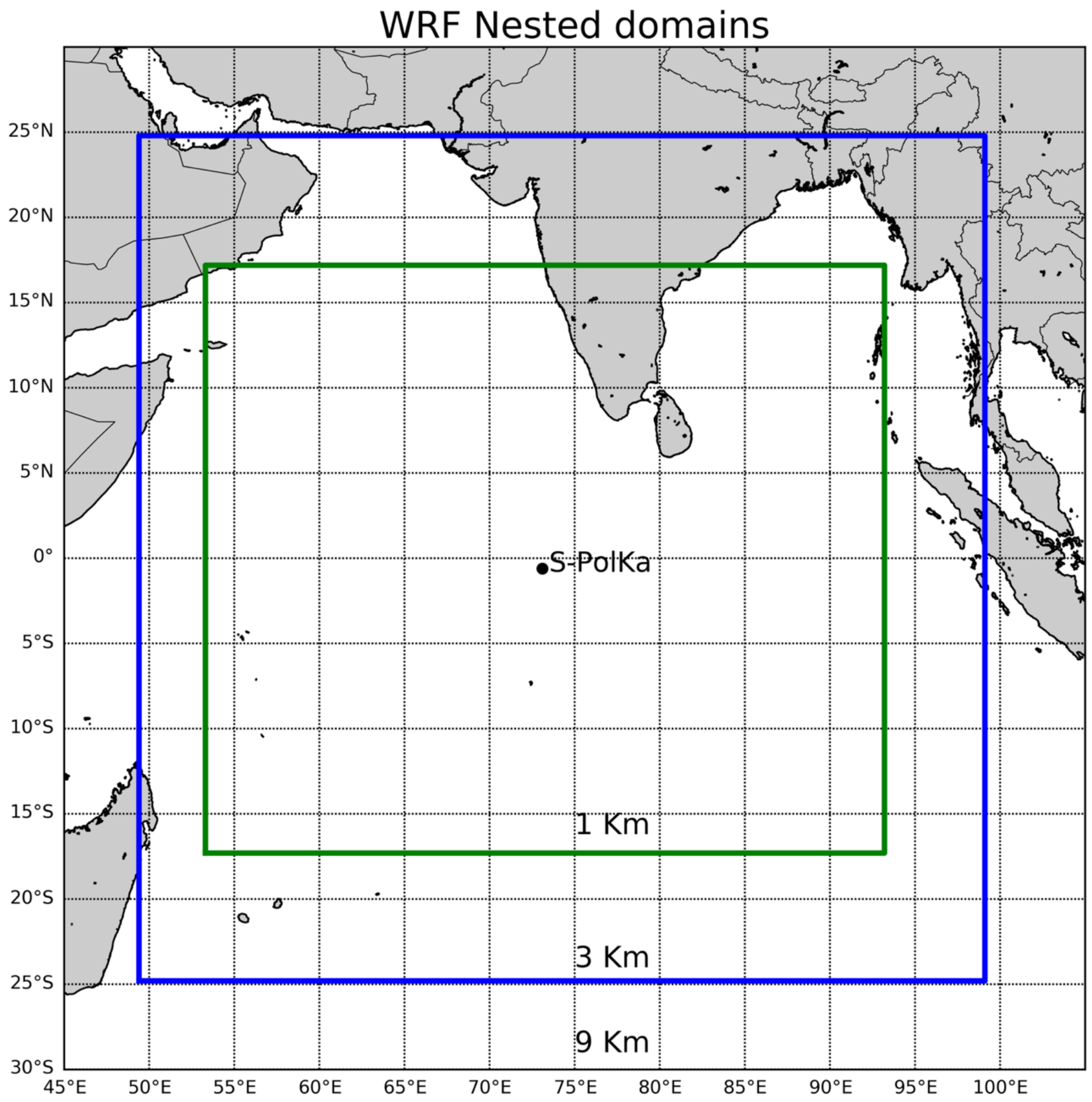

Horizontal Wind Gradient (s^{-1}) and Virtual Temperature Anomaly (K) on 18Z 01 November 2011

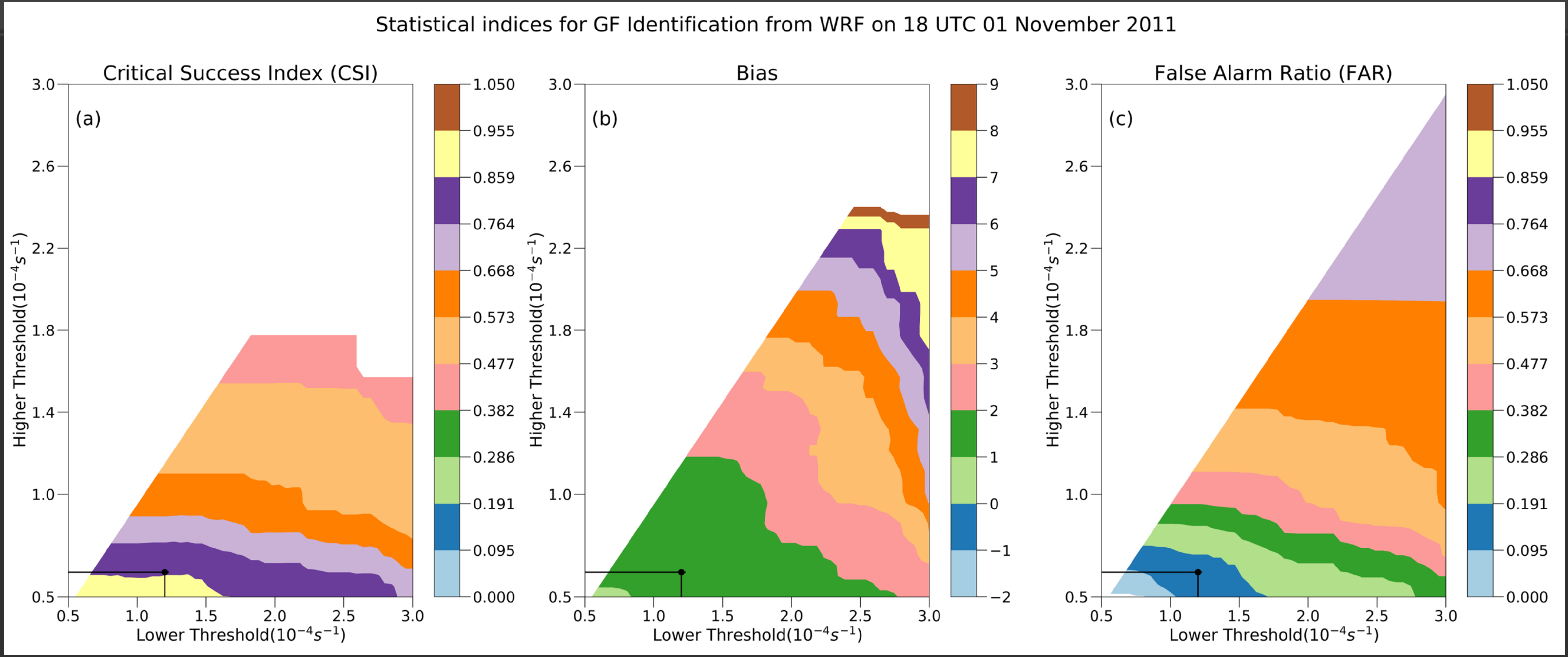

Buoy Validation Results

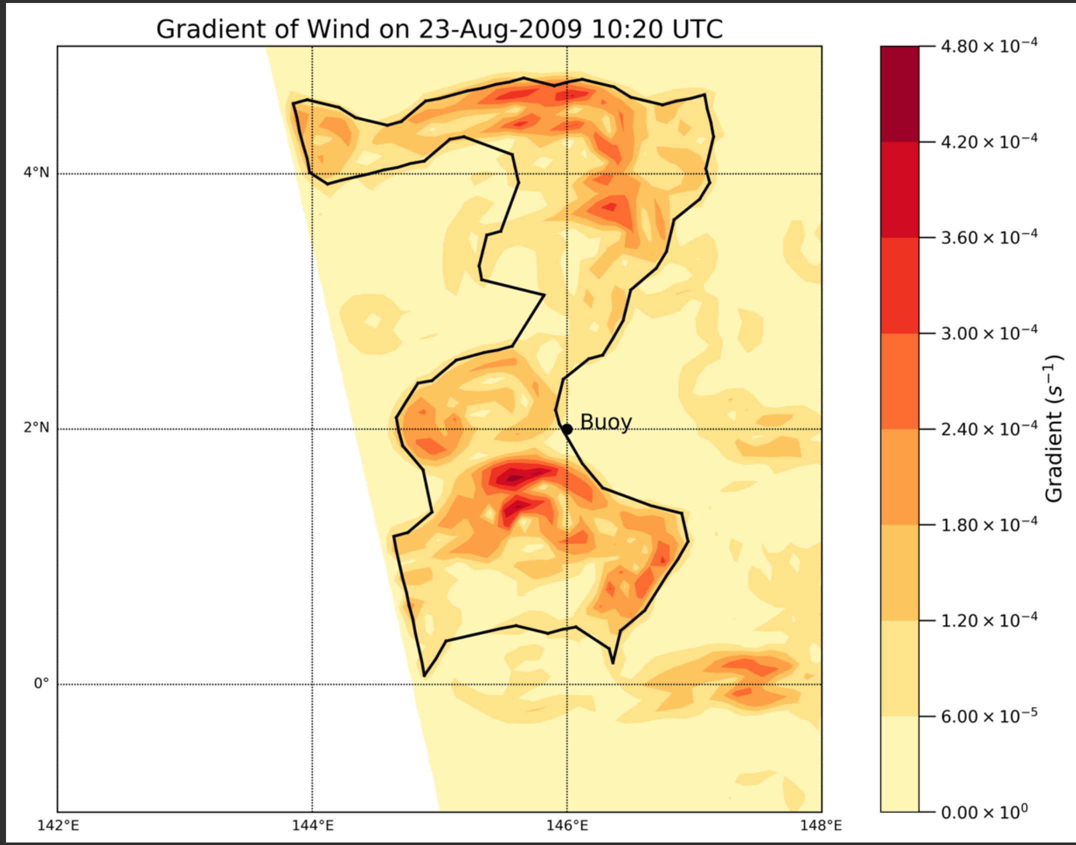

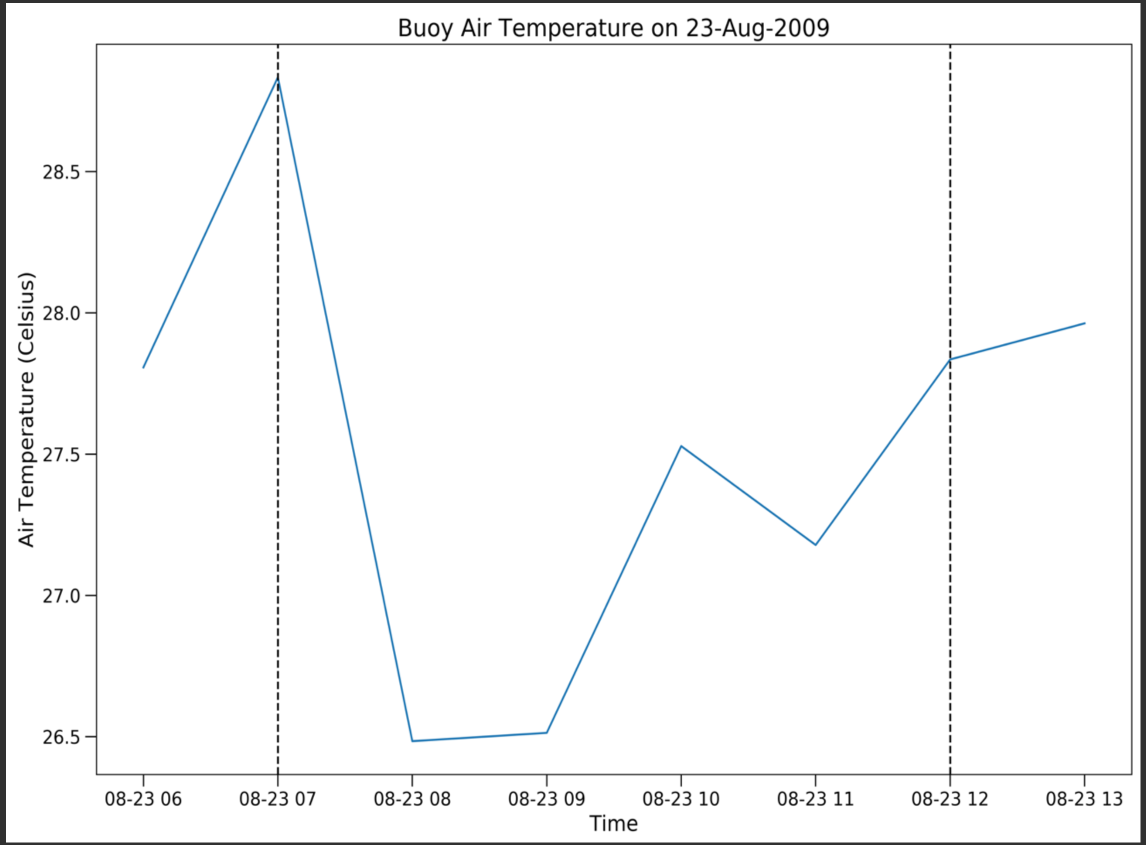

Buoys used for GF validation

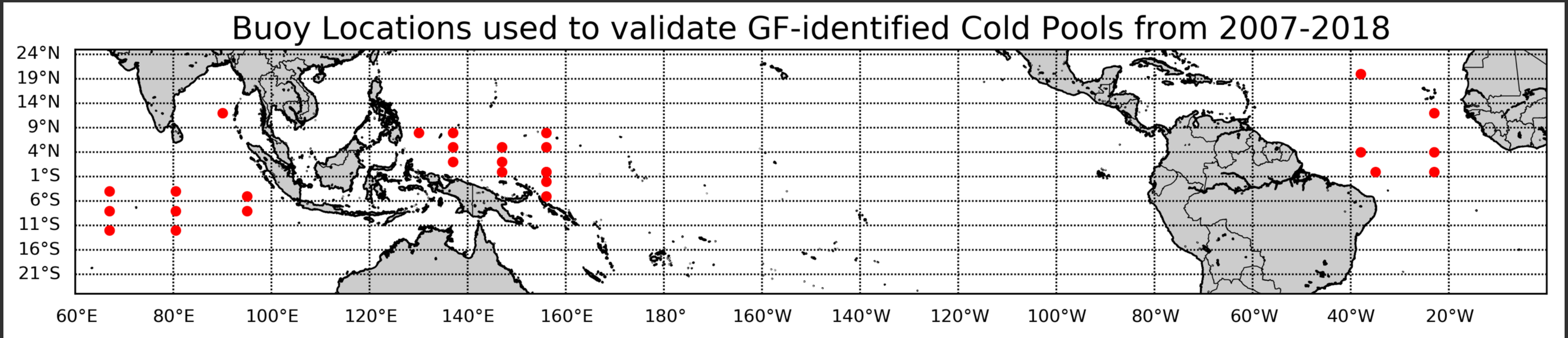

Thermal Cold Pools are identified if:
(Kilpatrick et al., 2015)

$$\begin{cases} T(t+1) - T(t) \geq -1.5\ ^{o}C \\ T(t+2) - T(t) \geq -2\ ^{o}C \end{cases}$$

Gradient Features (GFs) Polygon Buffer

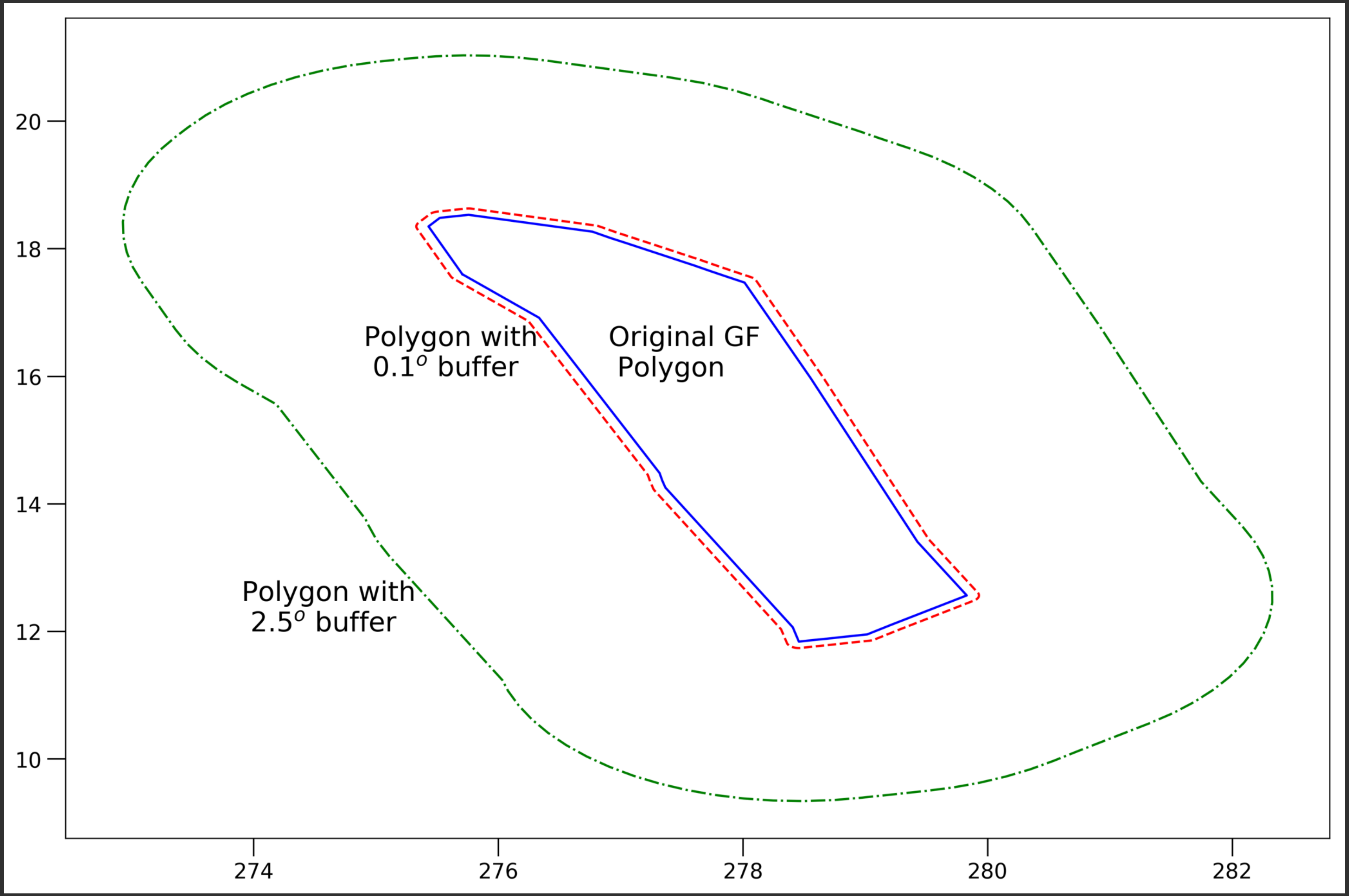

Gradient Feature (GF)

Air Temperature (T)

		YES	NO
	YES	A = Hits (If GF exists within the thermal cold pool period)	B = Missed events (No GF Present even though a thermal cold pool exists)
	NO	C = False alarms (GF is present although no thermal cold pool exists).	D = Correct rejections (Both the parameters don't have a cold pool)

Calculation of Success Indices from Buoys

Probability of Detection

$$POD = \frac{A}{A+B}$$

False Alarm Ratio

$$FAR = \frac{C}{(A+C)}$$

Success Ratio

$$SR = 1 - FAR$$

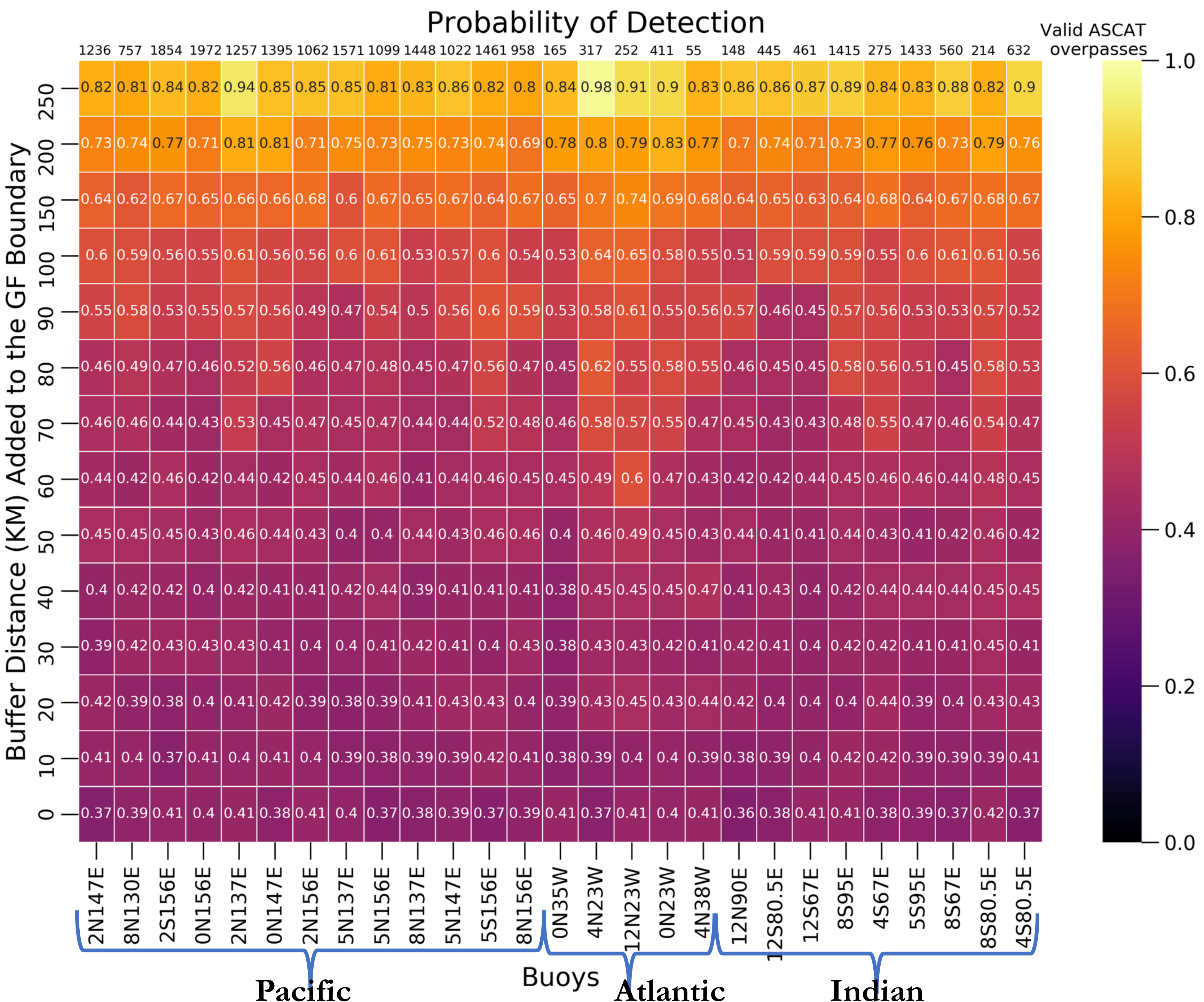

Probability of Detection
Valid ASCAT overpasses
1236 757 1854 1972 1257 1395 1062 1571 1099 1448 1022 1461 958 165 317 252 411 55 148 445 461 1415 275 1433 560 214 632
250 0.82 0.81 0.84 0.82 0.94 0.85 0.85 0.85 0.81 0.83 0.86 0.82 0.8 0.84 0.98 0.91 0.9 0.83 0.86 0.86 0.87 0.89 0.84 0.83 0.88 0.82 0.9
200 0.73 0.74 0.77 0.71 0.81 0.81 0.71 0.75 0.73 0.75 0.73 0.74 0.69 0.78 0.8 0.79 0.83 0.77 0.7 0.74 0.71 0.73 0.77 0.76 0.73 0.79 0.76
150 0.64 0.62 0.67 0.65 0.66 0.66 0.68 0.6 0.67 0.65 0.67 0.64 0.67 0.65 0.7 0.74 0.69 0.68 0.64 0.65 0.63 0.64 0.68 0.64 0.67 0.68 0.67
100 0.6 0.59 0.56 0.55 0.61 0.56 0.56 0.6 0.61 0.53 0.57 0.6 0.54 0.53 0.64 0.65 0.58 0.55 0.51 0.59 0.59 0.59 0.55 0.6 0.61 0.61 0.56
90 0.55 0.58 0.53 0.55 0.57 0.56 0.49 0.47 0.54 0.5 0.56 0.6 0.59 0.53 0.58 0.61 0.55 0.56 0.57 0.46 0.45 0.57 0.56 0.53 0.53 0.57 0.52
80 0.46 0.49 0.47 0.46 0.52 0.56 0.46 0.47 0.48 0.45 0.47 0.56 0.47 0.45 0.62 0.55 0.58 0.55 0.46 0.45 0.45 0.58 0.56 0.51 0.45 0.58 0.53
70 0.46 0.46 0.44 0.43 0.53 0.45 0.47 0.45 0.47 0.44 0.44 0.52 0.48 0.46 0.58 0.57 0.55 0.47 0.45 0.43 0.43 0.48 0.55 0.47 0.46 0.54 0.47
60 0.44 0.42 0.46 0.42 0.44 0.42 0.45 0.44 0.46 0.41 0.44 0.46 0.45 0.45 0.49 0.6 0.47 0.43 0.42 0.42 0.44 0.45 0.46 0.46 0.44 0.48 0.45
50 0.45 0.45 0.45 0.43 0.46 0.44 0.43 0.4 0.4 0.44 0.43 0.46 0.46 0.4 0.46 0.49 0.45 0.43 0.44 0.41 0.41 0.44 0.43 0.41 0.42 0.46 0.42
40 0.4 0.42 0.42 0.4 0.42 0.41 0.41 0.42 0.44 0.39 0.41 0.41 0.41 0.38 0.45 0.45 0.45 0.47 0.41 0.43 0.4 0.42 0.44 0.44 0.44 0.45 0.45
30 0.39 0.42 0.43 0.43 0.43 0.41 0.4 0.4 0.41 0.42 0.41 0.4 0.43 0.38 0.43 0.43 0.42 0.41 0.42 0.41 0.4 0.42 0.42 0.41 0.41 0.45 0.41
20 0.42 0.39 0.38 0.4 0.41 0.42 0.39 0.38 0.39 0.41 0.43 0.43 0.4 0.39 0.43 0.45 0.43 0.44 0.42 0.4 0.4 0.4 0.44 0.39 0.4 0.43 0.43
10 0.41 0.4 0.37 0.41 0.4 0.41 0.4 0.39 0.38 0.39 0.39 0.42 0.41 0.38 0.39 0.4 0.4 0.39 0.38 0.39 0.4 0.42 0.42 0.39 0.39 0.39 0.41
0 0.37 0.39 0.41 0.4 0.41 0.38 0.41 0.4 0.37 0.38 0.39 0.37 0.39 0.41 0.37 0.41 0.4 0.41 0.36 0.38 0.41 0.41 0.38 0.39 0.37 0.42 0.37
Buffer Distance (KM) Added to the GF Boundary
2N147E 8N130E 2S156E 0N156E 2N137E 0N147E 2N156E 5N137E 5N156E 8N137E 5N147E 5S156E 8N156E 0N35W 4N23W 12N23W 0N23W 4N38W 12N90E 12S80.5E 12S67E 8S95E 4S67E 5S95E 8S67E 8S80.5E 4S80.5E
Buoys
Pacific
Atlantic
Indian
1.0
0.8
0.6
0.4
0.2
0.0

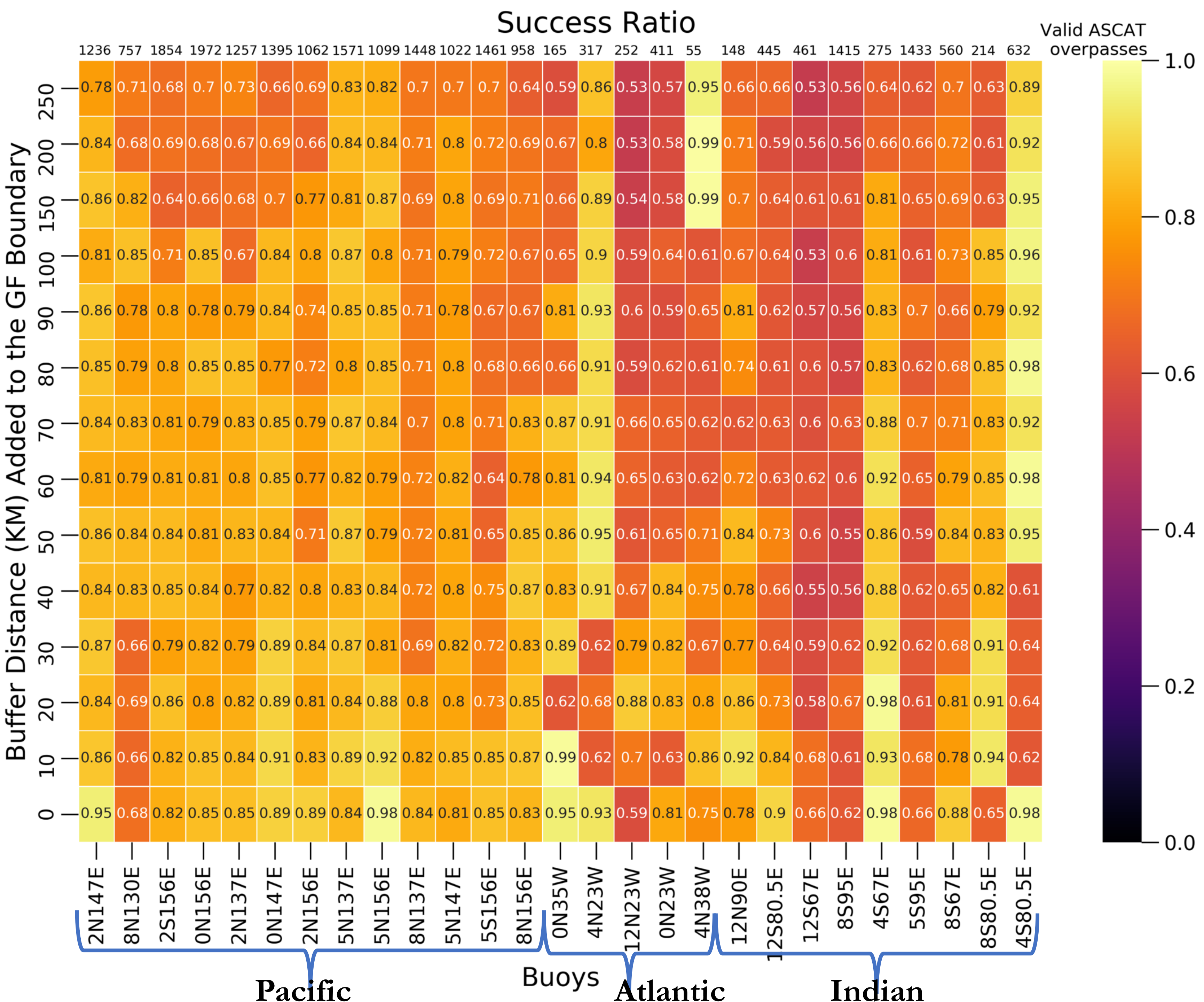

Success Ratio
Valid ASCAT overpasses
1236 757 1854 1972 1257 1395 1062 1571 1099 1448 1022 1461 958 165 317 252 411 55 148 445 461 1415 275 1433 560 214 632
250 0.78 0.71 0.68 0.7 0.73 0.66 0.69 0.83 0.82 0.7 0.7 0.7 0.64 0.59 0.86 0.53 0.57 0.95 0.66 0.66 0.53 0.56 0.64 0.62 0.7 0.63 0.89
200 0.84 0.68 0.69 0.68 0.67 0.69 0.66 0.84 0.84 0.71 0.8 0.72 0.69 0.67 0.8 0.53 0.58 0.99 0.71 0.59 0.56 0.56 0.66 0.66 0.72 0.61 0.92
150 0.86 0.82 0.64 0.66 0.68 0.7 0.77 0.81 0.87 0.69 0.8 0.69 0.71 0.66 0.89 0.54 0.58 0.99 0.7 0.64 0.61 0.61 0.81 0.65 0.69 0.63 0.95
100 0.81 0.85 0.71 0.85 0.67 0.84 0.8 0.87 0.8 0.71 0.79 0.72 0.67 0.65 0.9 0.59 0.64 0.61 0.67 0.64 0.53 0.6 0.81 0.61 0.73 0.85 0.96
90 0.86 0.78 0.8 0.78 0.79 0.84 0.74 0.85 0.85 0.71 0.78 0.67 0.67 0.81 0.93 0.6 0.59 0.65 0.81 0.62 0.57 0.56 0.83 0.7 0.66 0.79 0.92
80 0.85 0.79 0.8 0.85 0.85 0.77 0.72 0.8 0.85 0.71 0.8 0.68 0.66 0.66 0.91 0.59 0.62 0.61 0.74 0.61 0.6 0.57 0.83 0.62 0.68 0.85 0.98
70 0.84 0.83 0.81 0.79 0.83 0.85 0.79 0.87 0.84 0.7 0.8 0.71 0.83 0.87 0.91 0.66 0.65 0.62 0.62 0.63 0.6 0.63 0.88 0.7 0.71 0.83 0.92
60 0.81 0.79 0.81 0.81 0.8 0.85 0.77 0.82 0.79 0.72 0.82 0.64 0.78 0.81 0.94 0.65 0.63 0.62 0.72 0.63 0.62 0.6 0.92 0.65 0.79 0.85 0.98
50 0.86 0.84 0.84 0.81 0.83 0.84 0.71 0.87 0.79 0.72 0.81 0.65 0.85 0.86 0.95 0.61 0.65 0.71 0.84 0.73 0.6 0.55 0.86 0.59 0.84 0.83 0.95
40 0.84 0.83 0.85 0.84 0.77 0.82 0.8 0.83 0.84 0.72 0.8 0.75 0.87 0.83 0.91 0.67 0.84 0.75 0.78 0.66 0.55 0.56 0.88 0.62 0.65 0.82 0.61
30 0.87 0.66 0.79 0.82 0.79 0.89 0.84 0.87 0.81 0.69 0.82 0.72 0.83 0.89 0.62 0.79 0.82 0.67 0.77 0.64 0.59 0.62 0.92 0.62 0.68 0.91 0.64
20 0.84 0.69 0.86 0.8 0.82 0.89 0.81 0.84 0.88 0.8 0.8 0.73 0.85 0.62 0.68 0.88 0.83 0.8 0.86 0.73 0.58 0.67 0.98 0.61 0.81 0.91 0.64
10 0.86 0.66 0.82 0.85 0.84 0.91 0.83 0.89 0.92 0.82 0.85 0.85 0.87 0.99 0.62 0.7 0.63 0.86 0.92 0.84 0.68 0.61 0.93 0.68 0.78 0.94 0.62
0 0.95 0.68 0.82 0.85 0.85 0.89 0.89 0.84 0.98 0.84 0.81 0.85 0.83 0.95 0.93 0.59 0.81 0.75 0.78 0.9 0.66 0.62 0.98 0.66 0.88 0.65 0.98
Buffer Distance (KM) Added to the GF Boundary
2N147E 8N130E 2S156E 0N156E 2N137E 0N147E 2N156E 5N137E 5N156E 8N137E 5N147E 5S156E 8N156E 0N35W 4N23W 12N23W 0N23W 4N38W 12N90E 12S80.5E 12S67E 8S95E 4S67E 5S95E 8S67E 8S80.5E 4S80.5E
Pacific
Buoys
Atlantic
Indian
1.0
0.8
0.6
0.4
0.2
0.0

Global Climatology of ASCAT-Identified Cold Pools

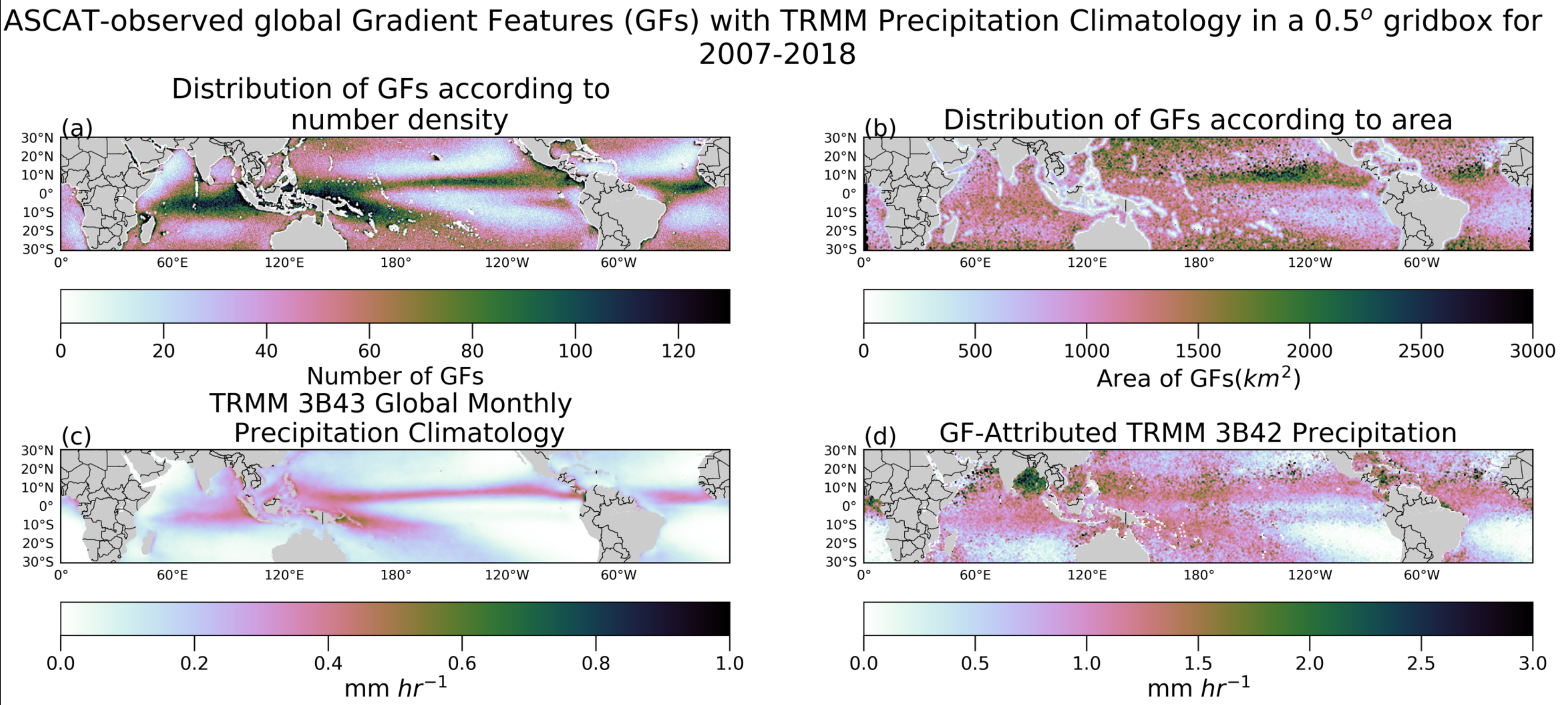

Summary and Conclusions

- GF technique is able to identify pockets of mesoscale downdrafts corresponding to tropical oceanic convective systems.

- WRF-simulated wind gradient-identified cold pools match well with thermal cold pools.

- ASCAT-identified gradient features validates well with in-situ buoy-identified thermal cold pools over tropical Indian, Pacific and Atlantic Ocean.

- Global climatology of GFs (Number) is corresponding well with TRMM precipitation, thus providing evidence that GFs are related to parent convective signatures.

Questions?

Delaunay Triangulation and Alpha Shapes

Mathematically, Delaunay triangulation says that for a set P of points in d-dimensional Euclidian space, no point in P is inside the circum-hypersphere of any d-simplex.

Alpha Shape is the concave hull of the triangulated polygon to give the connected outer edges of the polygon.

Delaunay Triangulation

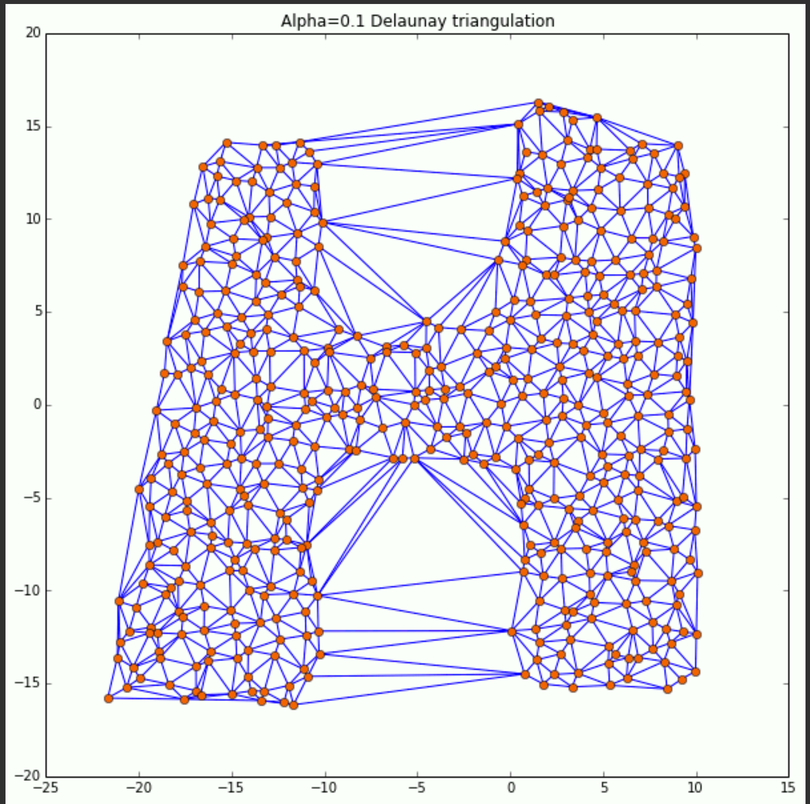

Source: Kevin Dwyer, HumanGeo blog

Alpha Shape

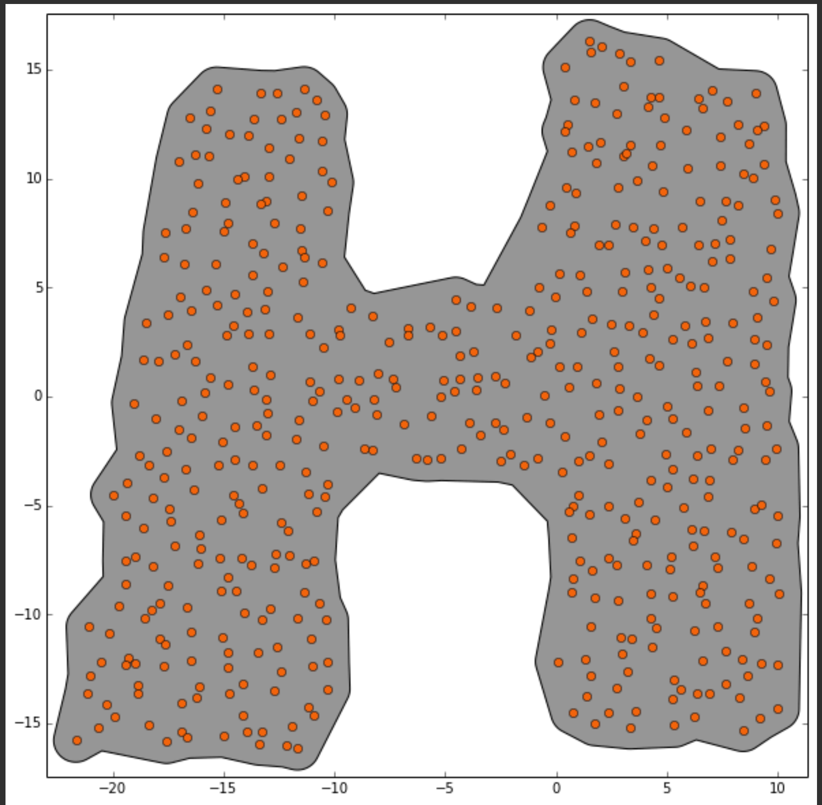

Source: Kevin Dwyer, HumanGeo blog

Gradient Feature (GF)

Virtual Temperature (T_v)

	YES	**NO**
YES	A = Hits (Intersection of GF and T_v is >= 50% of area of T_v)	B = Missed events (Intersection of GF and T_v is < 50% of the area of T_v)
NO	C = False alarms (No intersection between GF and T_v).	D = Correct rejections (Both the parameters don't have a cold pool)

Calculation of Success Indices from WRF

Critical Success Index

$$CSI = \frac{A}{(A+B+C)}$$

False Alarm Ratio

$$FAR = \frac{C}{(A+C)}$$

$$Bias = \frac{(A+B)}{(A+C)}$$